

Received March 18, 2021, accepted April 24, 2021, date of publication May 4, 2021, date of current version May 24, 2021.

Digital Object Identifier 10.1109/ACCESS.2021.3077267

Deep Learning Based Predictive Power Allocation for V2X Communication

JIAN SANG^{1,2}, TING ZHOU^{1,2}, (Member, IEEE), TIANHENG XU^{1,2}, (Member, IEEE),
YANLIANG JIN¹, (Member, IEEE), AND ZHENGHANG ZHU²

¹School of Communication and Information Engineering, Shanghai University, Shanghai 200444, China

²Shanghai Advanced Research Institute, Chinese Academy of Sciences, Shanghai 201210, China

Corresponding author: Ting Zhou (zhouting@sari.ac.cn)

This work was supported in part by the National Key Research and Development Program of China under Grant 2018YFB1802300, in part by the National Natural Science Foundation of China under Grant 61801461, and in part by the Shanghai Municipality of Science and Technology Commission Project under Grant 19511103102 and Grant 20JC1416500.

ABSTRACT As an essential technology of the fifth generation communication (5G), Vehicle-to-Everything (V2X) has attracted wide attention lately. A well-designed power allocation scheme can decrease the interference among terminals to yield a significant performance gain for V2X communication. Accurate channel state information (CSI) feedback, which is crucial to power allocation, is hard to be tracked due to fast time-varying channel in V2X scenario. This paper investigates power allocation problem under delayed CSI feedback in V2X system. We focus on maximizing sum throughput of V2X system while meeting Quality of Service (QoS) constraint requirement of each link. First of all, a power allocation scheme utilizing projective constraint analysis (PCA) is proposed to guarantee reliability of V2X network and improve system throughput, namely PCA-PA. Subsequently, we develop a Deep Neural Network (DNN) based predictive power allocation algorithm, namely DNN-PPA. This algorithm aims to address delayed CSI feedback in V2X system utilizing the normalized data obtained from PCA-PA scheme. Furthermore, a V2X communication model compliant with the 3rd Generation Partnership Project (3GPP) standard is simulated to validate the performances of PCA-PA and DNN-PPA. Simulation results illustrate that PCA-PA has superior performances compared to existing power allocation approaches and the throughput performance of DNN-PPA is impressively close to optimal solution under delayed CSI feedback.

INDEX TERMS V2X, power allocation, delayed CSI feedback, DNN.

I. INTRODUCTION

With the development of the fifth generation (5G) communication technology, Vehicle-to-Everything (V2X), which focuses on improving road safety and traffic efficiency for high-speed vehicles, is progressing rapidly [1]–[4]. Due to its advantages such as short-distance transmission and high reliability, V2X is considered as a typical scenario for Ultra Reliable Low Latency Communication (URLLC) of 5G. The 3rd Generation Partnership Project (3GPP) provides standards to enable highly efficient and reliable vehicular communications in future V2X networks [5].

Compared to traditional communication, V2X suffers from more intractable problems [6]–[11]. Firstly, the high-speed mobility of vehicle makes it difficult to capture accurate channel states information (CSI) feedback. Although the base

station (BS) samples the CSI, real-time sampling data is hard to be tracked because of fast time-varying channels. In brief, V2X has severe delay of CSI feedback [12]–[14]. Secondly, to improve spectral efficiency, Vehicle-to-Vehicle (V2V) links and Vehicle-to-Infrastructure (V2I) links share the same spectrum resources in a V2X system. However, this increases the interference among different links in the same spectrum although the spectral utilization is improved. Therefore, a well-designed interference management and power allocation scheme is an urgent requirement for V2X networks. Thirdly, some crucial QoS requirements are encountered for V2X communication, such as reliability [6], [15], [16]. This means that each link has to satisfy the minimum QoS constraint. Based on the above analysis, power allocation under delayed CSI feedback for V2X communication is an indispensable subject to be investigated.

Up to now, considerable researches have been conducted to address the challenges of power allocation for

The associate editor coordinating the review of this manuscript and approving it for publication was Moayad Aloqaity¹.

V2X communication [6], [17]–[22]. In [6], Liang *et al.* proposed a power allocation scheme, which improved the throughput of V2I link as much as possible while satisfying the QoS constraint of V2V link. In particular, the authors assumed the large-scale fading was updated every few hundred milliseconds and the small-scale fading took the long-term average. Based on [6], in [20] Wang *et al.* considered to maximize the sum position ergodic capacity in a highway scenario, which demands to maintain high throughput all along the way instead of instantaneous resource allocation. Reference [21] applied difference of two convex functions programming to obtain the optimal transmit power in a full CSI scenario. In [22], the power allocation problem under delayed CSI feedback was converted into convex expression by successive convex approximation.

With the development of research methods, the V2X challenges have been addressed through various technologies, including blockchain, artificial intelligence (AI) and so on [23]–[27]. In [23], Lin *et al.* considered a blockchain-based on-demand resource management, which constructed a two-stage Stackelberg game and solved resource allocation problem in V2X system creatively. In [24], Liang *et al.* proposed a micro-blockchain based geographical dynamic intrusion detection technology and enhanced the security of V2X.

In recent years, as AI is rising, deep learning (DL) has made great progress in wireless communication, such as environmental detection and mobile Internet of Things (mIoT) [28]–[32]. In [31], Khan *et al.* proposed an energy-efficient system based on DL with a real-time processing, which addressed the challenges of early smoke detection and provided support for DL-based V2X technology. In [32], Zafar *et al.* proposed Threshold Percentage Dependent Interference Graph using DL-based resource allocation algorithm for city buses mounted with moving small cells (mSCs). It provided a direction for DL to solve the resource allocation problem in mobile communication network.

DL utilizes numerous nonlinear layers to model high-level abstractions, which requires few manual calculations and provides the solutions for many complicated problems. Thus, the application of DL in V2X has also attracted extensive attention [33]–[36]. In [33], Ye *et al.* proposed a deep reinforcement learning based resource allocation scheme in V2X scenario. The authors took into account many channel characteristics, such as the instantaneous CSI and interference power, to train DL network. In [34], Lee *et al.* considered the wireless resource management optimization transforming to training tasks of the deep neural network (DNN). In [35], Gao *et al.* adopted weighted minimum mean square error (WMMSE) algorithm to acquire appropriate transmit power and then utilized instantaneous CSI to train DNN. The aforementioned DL-enabled power allocation schemes improve the performance of V2X system. However, there are still some practical problems such as dependence on instantaneous CSI feedback and neglect of

strict QoS constraints. In consequence, the power allocation schemes have unsatisfactory performance under delayed CSI feedback in high-speed V2X scenario and still require further research.

Motivated by such circumstances, in this paper a DL based predictive power allocation algorithm is developed under delayed CSI feedback in V2X scenarios. The proposed algorithm maximizes sum throughput of V2X system while guaranteeing reliability for each link. Especially, a V2X communication model based on 3GPP is simulated to validate the performance of proposed algorithm. The main contributions of this paper are summarized as follows:

a) We develop a power allocation scheme to maximize sum throughput of V2X system and guarantee QoS constraint of each link. The proposed scheme utilizes projective constraint analysis (PCA) to map the relation between throughput performance and power allocation, namely PCA-PA. On this base, we further derive a feasible region classification strategy of power allocation and formulate the corresponding optimal solution for V2X communication.

b) In order to solve the problem of delayed CSI feedback in V2X system, we propose a DNN based predictive power allocation algorithm, namely DNN-PPA. This algorithm is trained and tested by data set obtained from the PCA-PA scheme. The trained DNN-PPA algorithm utilizes statistical CSI characteristics of previous time slots to predict current optimal power allocation and requires no instantaneous CSI feedback.

c) Based on the 3GPP standard, we simulate a V2X channel model on the highway where performances of proposed PCA-PA and DNN-PPA are validated. Simulation results indicate that the PCA-PA scheme shows superior performances compared to existing approaches. Additionally, under delayed CSI feedback in V2X scenario, the throughput performance of DNN-PPA is outstandingly close to optimal solution.

The rest of this article is organized as follows. In Section II, the system model is described and the power allocation problem in V2X system is demonstrated mathematically. After that, We formulate the PCA-PA scheme to maximize system throughput and satisfy minimum QoS constraint in Section III. In Section IV, we present the network structure as well as training and testing phase of DNN-PPA. Simulation results and corresponding performance analysis are exhibited in Section V. Finally, we conclude our work in Section VI.

Nation: In this paper, the major nations are shown in Table 1.

II. SYSTEM MODEL AND PROBLEM FORMULATION

A. SYSTEM MODEL

Consider an uplink communication scenario in V2X system as shown in Fig. 1 [6]. Notably the contributions of this paper focus on the algorithm proposed for the V2X system. In order to ensure the generality, a widely studied V2X model is adopted. In Fig. 1, on one hand, V2I links exchange information between mobile vehicles and roadside infrastructure.

TABLE 1. The notation of symbol.

Symbol	Representative meaning
V2X	Vehicle-to-Everything
V2V	Vehicle-to-Vehicle
V2I	Vehicle-to-Infrastructure
VUE	Vehicle using V2V links
CUE	Vehicle using V2I links
QoS	Quality of service
CSI	Channel state information
PCA	Projective constraint analysis
DNN	Deep neural network
MRP	Maximum received power
MIP	Maximum interference power
MARP	Maximum acceptable interference power
MAIP	Minimum acceptable received power

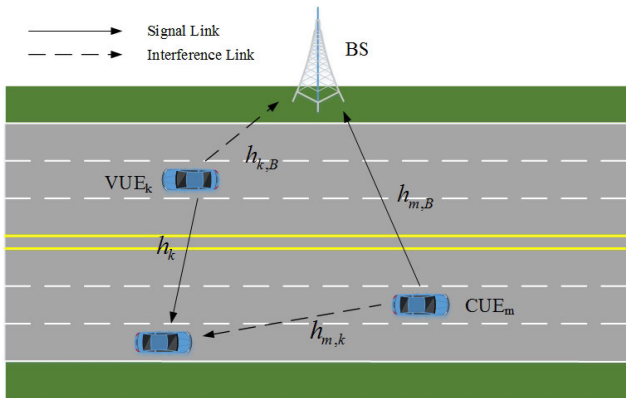


FIGURE 1. V2X communication scenario.

On the other hand, V2V links are utilized for information transmission between two mobile vehicles. Given that M vehicles communicate via V2I links, denoted as CUEs, and K pairs of vehicles propagate local data via V2V links, denoted as VUEs. We note that each vehicle is allowed to use only one link, i.e., V2V or V2I, to propagate data. The QoS constraint, expressed as minimum throughput threshold, is required for each link. Denote the CUE set as $\mathbf{M} = \{1, \dots, M\}$ and VUE set as $\mathbf{K} = \{1, \dots, K\}$. To improve spectrum utilization efficiency, orthogonally allocated uplink spectra of CUEs are reused by VUEs since uplink resources are less intensively used [6]. Especially, in order to reduce interference between VUEs and CUEs, we assume that the spectrum of one CUE can only be reused by a single VUE. In addition, one VUE is only allowed to share the spectrum of a single CUE.

The signal channel power gain $h_{m,B}$, between the m th CUE and BS, follows [5]

$$h_{m,B} = PL_{m,B} \beta_{m,B} g_{m,B}, \quad (1)$$

where $PL_{m,B}$ indicates the path loss between the m th CUE and BS, which depends on the positions of vehicles. $\beta_{m,B}$ denotes a log-normal shadow fading random variable with a standard deviation ξ . $g_{m,B}$ is the small-scale fast fading power component and the Jakes model of Rayleigh fading is adopted in this paper. Due to the high-speed mobility of vehicles, we assume that both large scale fading and small scale fading

change rapidly over time. Signal channel h_k between the k th pair of VUEs, interference channel $h_{k,B}$ between the k th VUE and BS, and interference channel $h_{m,k}$ between the m th CUE and the k th VUE are similarly defined.

Respectively, received signal to interference plus noise ratio (SINR) at BS of the m th CUE and at the k th VUE can be expressed as

$$\gamma_m = \frac{P_m h_{m,B}}{\sigma^2 + \rho_{m,k} P_k h_{k,B}}, \quad (2)$$

and

$$\gamma_k = \frac{P_k h_k}{\sigma^2 + \rho_{m,k} P_m h_{m,k}}, \quad (3)$$

where P_m and P_k denote transmit powers of the m th CUE and the k th VUE. σ^2 denotes noise power. $\rho_{m,k}$ is the spectrum reusing indicator with $\rho_{m,k} = 1$ indicating spectrum of the m th CUE is reused by the k th VUE and $\rho_{m,k} = 0$ otherwise. The throughput of the m th CUE is given by

$$C_m = \log_2(1 + \gamma_m). \quad (4)$$

The throughput of the k th VUE is similarly defined.

B. PROBLEM FORMULATION

In a V2X uplink communication aiming to maximize system throughput, the throughput of each link needs to exceed the minimum constraint in order to guarantee QoS. However, when improving throughput, each vehicle tends to increase its transmit power, which in turn increases interference to the other link in the reusing channel. Therefore, there exists a trade-off between transmit powers of vehicles, which needs to be leveraged in power allocation. Our goal is to develop an optimal power allocation solution to maximize system throughput while guaranteeing the QoS constraint of each link. In consequence, with the definitions of throughput in (4), the power allocation problem can be formulated as follows.

$$(P_k, P_m) = \arg \max [\log_2(1 + \gamma_k) + \log_2(1 + \gamma_m)] \quad (5)$$

$$s.t. \log_2(1 + \gamma_k) \geq \lambda \quad (5a)$$

$$\log_2(1 + \gamma_m) \geq \lambda \quad (5b)$$

$$0 \leq P_k \leq P_{\max} \quad (5c)$$

$$0 \leq P_m \leq P_{\max} \quad (5d)$$

$$\rho_{m,k} \in \{0, 1\}, \forall m \in \mathbf{M}, \forall k \in \mathbf{K}, \quad (5e)$$

where λ is the minimum throughput threshold to meet QoS constraint, P_{\max} represents the maximum transmit power of vehicle. Equation (5) mathematically represents the objective function, which is the power allocation design in spectrum reusing mode to maximize the system throughput and satisfy the QoS constraints of all V2X links. Constraints (5a) and (5b) indicate the minimum throughput requirements for each CUE and VUE, respectively. (5c) and (5d) ensure that the transmit powers of CUEs and VUEs cannot exceed the maximum limit. (5e) mathematically models our assumption that the spectrum of one CUE can only be reused by a single VUE and one VUE is only allowed to share the spectrum of a

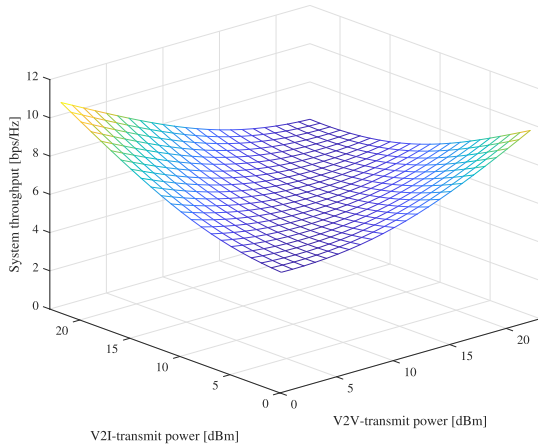


FIGURE 2. System throughput without QoS constraint versus power allocation.

single CUE. This assumption improves spectrum utilization and reduces the complexity, which provides a promising framework for power allocation in V2X network.

The objective function as described in (5) is a function of power allocation under channel gain combinations of V2I and V2V links. Therefore, based on channel gains, we consider a PCA method and formulate the optimal solution to tackle power allocation problem visually in Section III. In addition, a predictive power allocation scheme based on DL is proposed in order to address delayed CSI feedback for V2X system in Section IV.

III. DESIGN OF PCA-PA SCHEME

In this section, first we intuitively analyze the power allocation feasible region for (5) using a PCA method. On basis of the first step, we further propose a feasible region classification strategy and provide the optimal power allocation solution to maximize system throughput while satisfying QoS constraint for each link.

A. PCA METHOD

In the uplink communication of V2X system, we map the relation between throughput performance and power allocation from three-dimensional space to two-dimensional plane. The details of PCA are shown in Fig. 2 and Fig. 3. Fig. 2 illustrates the relationship between unconstrained throughput plain of V2X and power allocation under certain channel gains. Obviously, this plain is continuous in the global solution space with power allocation (P_k, P_m) . In Fig. 3(a) and Fig. 3(b), taking account into QoS constraints, the plains of throughput and portions of power allocation region are shown for V2I and V2V links respectively. As we can see, the throughput of V2I link increases monotonically with a growing transmit power of CUE, but decreases monotonically as VUE increases transmit power. However, the throughput of V2V link shows a completely opposite trend. As a result, there is a throughput trade off between V2I and V2V links. In Fig. 3(c), the V2X system throughput under two QoS constraints and corresponding power allocation por-

Algorithm 1 The Algorithm for Classification Cases in Fig. 4

- 1 Acquire the CSI, $h_{m,B}, h_k, h_{k,B}, h_{m,k}$.
- 2 MRPs of the m th CUE and k th VUE, i.e., $(P_{\max}h_{m,B})$ and $(P_{\max}h_k)$, as well as MIPs of the m th CUE and k th VUE, i.e., $(P_{\max}h_{k,B})$ and $(P_{\max}h_{m,k})$, are deduced accordingly.
- 3 According to λ , the corresponding SINRs of m th CUE and k th VUE, i.e., γ_m and γ_k are deduced by (5a) and (5b) respectively.
- 4 Substituting MRP of the m th CUE into (2), MAIP of the m th CUE can be inferred, i.e., $P_{k,B}^* = \frac{P_{\max}h_{m,B} - \gamma_m \sigma^2}{\gamma_m h_{k,B}}$.
- 5 MAIP of the k th VUE $P_{m,k}^*$, MARP of the m th CUE $P_{m,B}^*$ and MARP of the k th VUE P_k^* can be derived similarly.
- 6 **if** $0 < P_{k,B}^* < P_{\max}$ & $P_k^* < P_{k,B}^*$ **then**
Case I.
- 7 **elseif** $0 < P_{m,k}^* < P_{\max}$ & $P_{m,B}^* < P_{m,k}^*$ **then**
Case II.
- 8 **elseif** $P_k^* < P_{\max}$ & $P_{m,B}^* < P_{\max}$ **then**
Case III.
- 9 **else**
Case IV.
- 10 **end**

tion are shown. Compared with Fig. 2, it is obvious that only part of power allocation region satisfies the condition of (5). According to the feasible region, the optimal solution of (5) can be obtained in a limited plain as illustrated in Fig. 3(d). Unfortunately, such a feasible region is irregularly distributed and should be decided by quantitative value of channel gains, i.e., $\{h_{m,B}, h_k, h_{k,B}, h_{m,k}\}$. Therefore, based on channel gains, we explore the optimal solution of feasible region for (5) using a classification strategy in the subsection III-B.

B. PCA-PA APPROACH

As mentioned above, the feasible region of power allocation is determined by quantitative value for channel gains. Therefore, we classify the feasible region cases to explore the position of optimal solution for (5). In Algorithm 1, we present the classification algorithm according to the maximum received power (MRP), maximum interference power (MIP), maximum acceptable interference power (MAIP) and minimum acceptable received power (MARP) of V2X system. In particular, MRP represents the maximum received power at receiver in signal channel when P_{\max} is applied at transmitter. MIP represents the maximum interference power at receiver in interference channel when P_{\max} is used at transmitter. MAIP denotes the maximum acceptable interference power for interference channel under satisfying QoS constraint, when the transmitter in signal channel is P_{\max} . MARP denotes the minimum acceptable

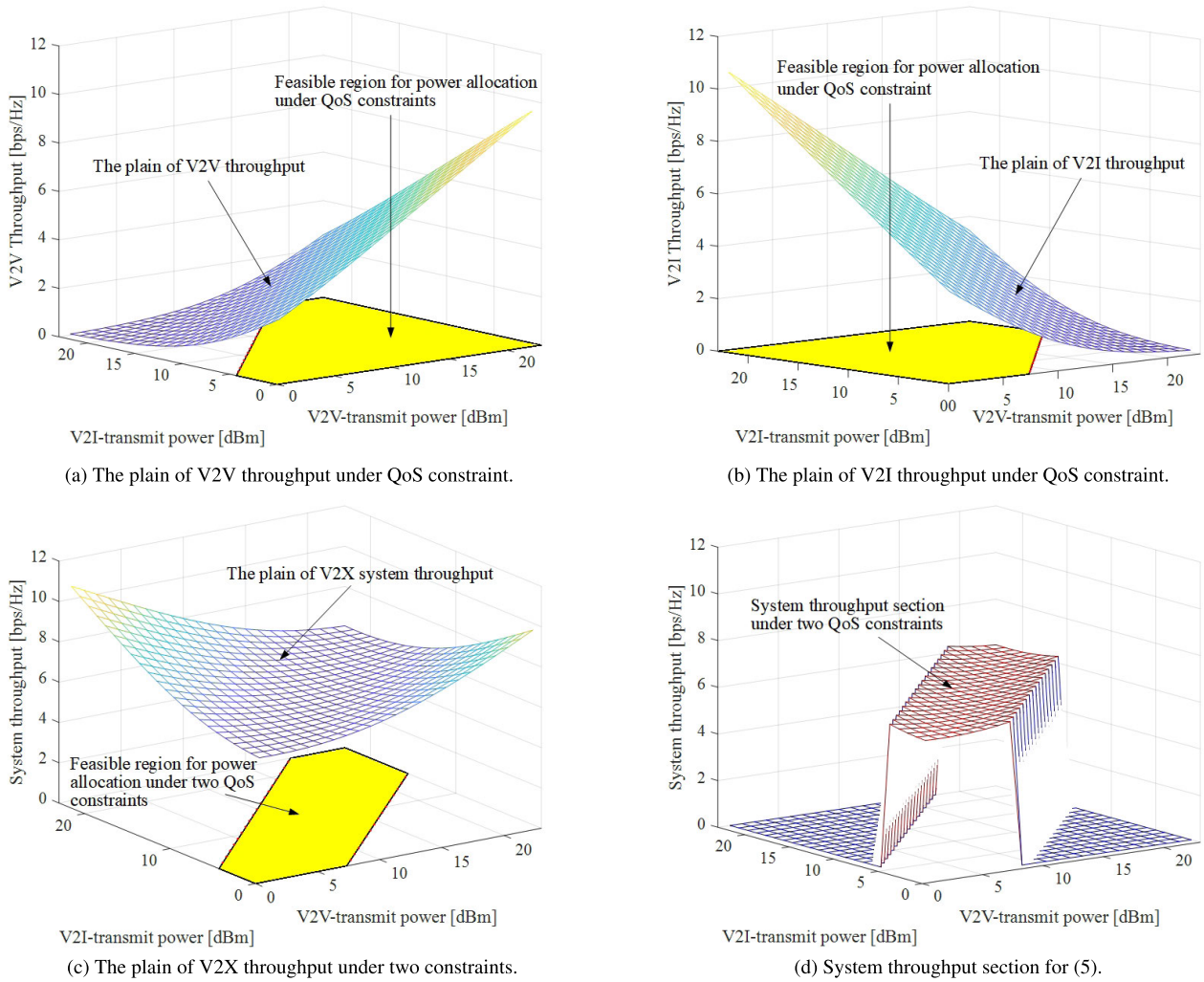


FIGURE 3. Projective constraint analysis for power allocation.

received power for signal channel under satisfying QoS constraint, when the transmitter in interference channel is P_{\max} . Additionally, Fig. 4 shows the classification cases in detail.

As shown in Fig. 4, taking account into distribution positions of feasible regions, power allocation solution for (5) can be classified into 4 cases. Consider the symmetry line of power allocation region, i.e., the line from (0, 0) to (23, 23), as baseline. The feasible region is completely above the baseline in Case I while oppositely below the baseline in Case II. For Case III, the feasible region is distributed on both sides of baseline. In contrast to Case I - III, Case IV depicts that in some harsh V2X communication scenarios, any power allocation (P_k, P_m) cannot meet QoS constraint, i.e., no power allocation solution for (5). Note that Fig. 4 only classifies distribution positions of feasible region for power allocation, rather than being accurate to numerical values. As mentioned above, the optimal solution for (5) depends on the quantitative values of channel gains. Therefore, based on classification cases, the optimal power allocation (P_k, P_m)

for (5) is further derived in the following theorems, proved in Appendix.

Theorem 1: The optimal solution for feasible power allocation region is given by

$$(P_k, P_m) = (P^*_{V2V}, P_{\max}), \quad (6)$$

or

$$(P_k, P_m) = (P_{\max}, P^*_{V2I}), \quad (7)$$

where P^*_{V2V} and P^*_{V2I} respectively represent the quantitative transmit powers of VUE and CUE under the maximum power limit. P_{\max} is the maximum transmit power. According to Theorem 1, in the optimal power allocation solution (P_k, P_m) , there exists at least one variable with the value of P_{\max} . This indicates that the optimal solution is located on the curve ‘A-B’ for Case I-III in Fig. 4. It is worth noting that according to Algorithm 1, A and B represent respectively (P^*_k, P_{\max}) and $(P^*_{k,B}, P_{\max})$ for Case I, $(P_{\max}, P^*_{m,B})$ and $(P_{\max}, P^*_{m,k})$ for Case II as well as (P^*_k, P_{\max}) and $(P_{\max}, P^*_{m,B})$ for Case III. Theorem 1 further reduces the

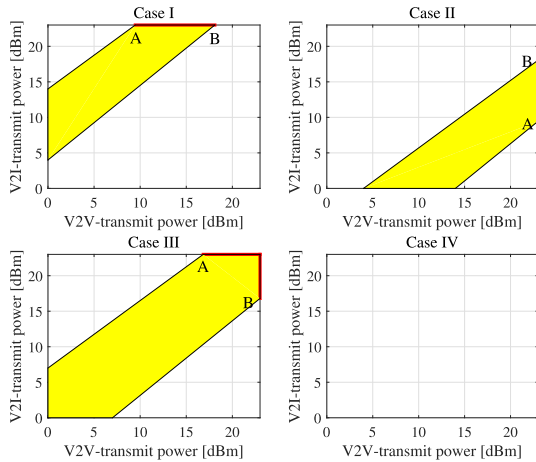


FIGURE 4. Classification cases of feasible region for (5).

optimal power allocation region and provides a direction for finding the optimal solution of (5). The rest is to discuss the value of another variable besides P_{\max} , i.e., P^*_{V2V} in (6) and P^*_{V2I} in (7).

Theorem 2: The optimal solutions for classification cases in Fig. 4 can be expressed as

$$\begin{aligned}
 \text{Case I} & : (P_k, P_m) = (P^*_{k,B}, P_{\max}) \\
 \text{Case II} & : (P_k, P_m) = (P_{\max}, P^*_{m,k}) \\
 \text{Case III} & : (P_k, P_m) = \arg \max (\Gamma) \\
 \text{Case IV} & : \text{No solution},
 \end{aligned} \tag{8}$$

where $\Gamma = \{C(P^*_k, P_{\max}), C(P_{\max}, P^*_{m,B})\}$ and $C(\bullet)$ represents system throughput function under corresponding power allocation. Respectively, $P^*_{k,B}$, $P^*_{m,k}$, P^*_k and $P^*_{m,B}$ are MAIP of the m th CUE, MAIP of the k th VUE, MARP of the k th VUE and MARP of the m th CUE, which are obtained from Algorithm 1. Equation (8) addresses the power allocation problem of (5) by providing the optimal solution of each classification case for aforementioned PCA-PA scheme. It should be noted that the 4 subformulas in (8) correspond to 4 classification cases respectively in Fig. 4.

From the above discussion, Algorithm 2 to find the optimal power allocation solution for (5) is summarized. Algorithm 2 calculates the MAIP of signal channel and MARP of interference channel for vehicles, including M CUEs and K VUEs. During this process, each vehicle is calculated twice by Algorithm 2. This leads to the total complexity of $O[2(K + M)]$ to determine the optimal power allocation for (5). Note that Algorithm 2 is a power allocation approach on the basis of CSI feedback, which is hard to be captured in V2X scenario. DNN can generate powerful characterization capabilities for the mapping relations between random vector units. It provides a direction for exploring channel gain variation in V2X scenarios. Therefore, in Section IV, we propose a predictive power allocation algorithm utilizing the data set obtained from PCA-PA scheme. The proposed

Algorithm 2 PCA-PA Scheme for (5)

- 1 Acquire the CSI, $h_{m,B}$, h_k , $h_{k,B}$, $h_{m,k}$.
- 2 Calculate the MRPs and MIPs.
- 3 Substitute MRPs and MIPs into (5) to derive MAIPs and MARPs, i.e., $P^*_{k,B}$, $P^*_{m,k}$, $P^*_{m,B}$, P^*_k .
- 4 Determine the feasible region classification case of power allocation by Algorithm 1.
- 5 **if** Case I **then**
 $(P_k, P_m) = (P^*_{k,B}, P_{\max})$.
- 6 **elseif** Case II **then**
 $(P_k, P_m) = (P_{\max}, P^*_{m,k})$.
- 7 **elseif** Case III **then**
 8 **if** $C(P^*_k, P_{\max}) < C(P_{\max}, P^*_{m,B})$ **then**
 $(P_k, P_m) = (P_{\max}, P^*_{m,B})$.
- 9 **else**
 $(P_k, P_m) = (P^*_k, P_{\max})$.
- 10 **end if**
- 11 **else**
 No optimal power allocation solution.
 $C = 0$.
- 12 **end if**
- 13 Upload the normalized CSI and optimal power allocation solution into data set.

algorithm aims to solve the problem of delayed CSI feedback by utilizing DNN.

IV. DESIGN OF DNN-PPA ALGORITHM

The PCA-PA scheme in Section III maximizes the system throughput while QoS constraints are satisfied, which provides the optimal solution for (5) on basis of CSI feedback. However, due to fast time-varying channels, V2X system suffers from delayed CSI feedback, which needs to be addressed. Consequently, for the power allocation under delayed CSI feedback, we consider a DNN, which utilizes Back Propagation neural network as its core. Notably DNN does not have the exploration ability of providing optimal power allocation for the objective function independently. Therefore, we need to provide the appropriate data set to fit the weight of DNN. The aforementioned PCA-PA scheme is on purpose of finding the optimal power allocation data under instantaneous CSI feedback and providing training data for DNN-PPA. Particularly, the statistical CSI characteristics of previous time slots are utilized for DNN-PPA without need for instantaneous CSI feedback. It is worth noting that the DNN consists of training phase and testing phase. In the training phase, massive data are fed into network to produce a trained model. In the testing phase, test data were used to verify prediction performance of trained DNN model.

A. DNN MODEL

The network structure of DNN is shown in Fig. 5. For ease of expression, we illustrate the network structure consisting of one input layer, one hidden layer and one output layer. In Fig. 5, $\{x_1, \dots, x_i, \dots, x_d\}$, $\{b_1, \dots, b_h, \dots, b_q\}$

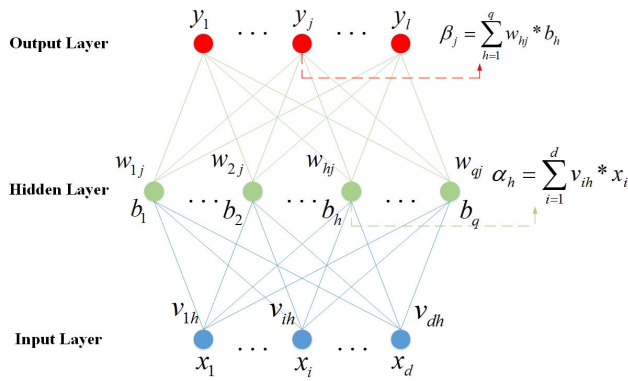


FIGURE 5. Network structure of DNN.

and $\{y_1, \dots, y_j, \dots, y_l\}$ denote respectively the network parameters of input layer, hidden layer and output layer. v_{ih} and w_{hj} are weights from input layer to hidden layer and from hidden layer to output layer. γ_h and θ_j respectively indicate thresholds of the h th neuron in hidden layer and the j th neuron in output layer. $b_h = f(\alpha_h - \theta_h)$, where α_h represents input of the h th neuron in hidden layer. β_j is input of the j th neuron in output layer. $f(\bullet)$ represents the Sigmoid function, which is adopted as the activation function from hidden layer to output layer and defined as

$$f(x) = \frac{1}{1 + e^{-x}}. \tag{9}$$

The error function between DNN output and target output is defined as

$$E_k = \frac{1}{2} \sum_{j=1}^l (y^{k'}_j - y^k_j)^2, \tag{10}$$

where $y^{k'}_j$ is DNN output and y^k_j is target output. Then we adopt the gradient descent method to adjust the weights v_{ih} and w_{hj} as well as the thresholds γ_h and θ_j , respectively.

The weight adjustment from hidden layer to output layer, Δw_{hj} , is defined as

$$\Delta w_{hj} = -\eta \frac{\partial E_k}{\partial w_{hj}}, \tag{11}$$

where η is learning rate.

Additionally, the threshold adjustment in output layer, $\Delta \theta_j$, is expressed as

$$\Delta \theta_j = -\eta \frac{\partial E_k}{\partial \theta_j}. \tag{12}$$

The weight adjustment from input layer to hidden layer and threshold adjustment in hidden layer are similarly defined.

B. DNN-PPA ALGORITHM

DNN consists of training phase and testing phase. The training phase can be regarded as a process of weight adjustment, which aims to explore the mapping relationship between input parameters and output parameters. The data sets used

TABLE 2. The data sets for DNN model.

Parameters	Value
VUE transmit power P_k	$\{0, 1, \dots, 23\}$ dBm
CUE transmit power P_m	$\{0, 1, \dots, 23\}$ dBm
CSI in signal channel for VUE	h_k
CSI in interference channel for VUE	$h_{m,k}$
CSI in signal channel for CUE	$h_{m,B}$
CSI in interference channel for CUE	$h_{k,B}$

Algorithm 3 DNN-PPA Algorithm.

- 1 Acquire the CSI feedback $h_{m,B}, h_k, h_{k,B}, h_{m,k}$.
- 2 Calculate the feasible region classification case of power allocation by **Algorithm 1**.
- 3 Calculate the optimal power allocation solution (P_k, P_m) by **Algorithm 2**.
- 4 Upload the normalized CSI and corresponding power allocation solutions (P_k, P_m) into training and testing data set.
- 5 Initialize the weights of DNN v_{ih}, w_{jh}, γ_h and θ_j .
- 6 Train DNN:
 - Repeat:**
 - Input the CSIs of previous n time slots and adjust the weights, $v_{ih}, w_{jh}, \gamma_h, \theta_j$ according to the error function of DNN.
 - Until** convergence
 - 7 Test DNN.
 - 8 Return trained DNN model and use it to predict power allocation.
 - 9 **end**

for DNN model training are extracted from PCA-PA scheme, which are shown in Table 2. From training data set, we select the statistical CSI characteristics of previous multiple time slots as inputs of DNN, which is defined as

$$x(t) = \{A(t - nt_0), A[t - (n - 1)t_0], \dots, A(t - t_0)\}, \tag{13}$$

where t_0 denotes one time slot, $A(t - nt_0)$ represents CSI before n time slots and follows

$$A(t - nt_0) = \begin{cases} h_k(t - nt_0) \\ h_{m,k}(t - nt_0) \\ h_{m,B}(t - nt_0) \\ h_{k,B}(t - nt_0) \end{cases} \tag{14}$$

Accordingly, the target outputs of DNN are the optimal power allocation solutions obtained by Algorithm 2, which can be denoted as follows. During the process, the weights of DNN are adjusted to fit the data sets.

$$y(t) = (P_k, P_m). \tag{15}$$

A large number of network parameters can easily lead to over-fitting, which limits its prediction performance. Therefore, in the work, we consider statistical CSI characteristics of previous n ($n < 10$) time slots as one sample. As a result, the input layer consists of $4n$ neurons. The hidden layers are considered as three layers and consist of 40, 40 and

TABLE 3. Simulation parameters [5], [6], [37], [38].

Parameter	Value	Parameter	Value
Number of lanes	3 in each direction (6 in total)	Lane width	4 m
Absolute vehicle speed	144 km/h	Distance between BS and highway	35 m
Vehicle drop model	Spatial Poisson Process	Carrier frequency f_c	5.9 GHz
Bandwidth	180 kHz	Noise power	-114 dBm
Number of VUEs	20	Number of CUEs	20
Vehicle antenna height h_{TX}	1.5 m	BS antenna height h_{BS}	25 m
Vehicle antenna gain	3 dBi	BS antenna gain	8 dBi
Vehicle receiver noise figure	9 dB	BS receiver noise figure	5 dB
Maximum VUE transmit power	23 dBm	Maximum CUE transmit power	23 dBm
Time delay	10 ms	Total number of time slots	1000
Length of single time slot	10 ms	Minimum QoS constraint	2 bps/Hz

TABLE 4. Channel models [37], [38].

Parameter	V2I link	V2V link
Path loss model	$PL_{LOS} = \begin{cases} PL_1, & 10 \text{ m} \leq d_{2D} \leq d_{BP} \\ PL_2, & d_{BP} \leq d_{2D} \leq 10 \text{ km} \end{cases}$ $PL_1 = 20 \log_{10} (40\pi d_{3D} f_c / 3) + \min(0.03h^{1.72}, 10) \log_{10} (d_{3D}) - \min(0.044h^{1.72}, 14.77) + 0.002 \log_{10}(h) d_{3D}$ $PL_2 = PL_1(d_{BP}) + 40 \log_{10} (d_{3D} / d_{BP})$	<p>LOS: $32.4 + 20 \log_{10} (d_{2D}) + 20 \log_{10} (f_c)$</p> <p>NLOS: $36.85 + 30 \log_{10} (d_{2D}) + 18.9 \log_{10} (f_c)$</p>
LOS probability	All V2I links are considered as line-of-sight scenarios.	$\begin{cases} P_1, & d_{2D} \leq 475 \\ P_2, & d_{2D} > 475 \end{cases}$ $P_1 = \min(1, a * d_{2D}^2 + b * d_{2D} + c)$ $P_2 = \max(0, 0.54 - 0.001 * (d_{2D} - 475))$ $a = 2.1013e - 6, b = -0.002, c = 1.0193$
Shadow distribution	Log-normal	Log-normal
Shadow standard deviation	8	3
Fast fading	Rayleigh fading	Rayleigh fading
Fast fading model	Jakes	Jakes

50 neurons respectively. The transmit powers of VUEs and CUEs are spaced at 1 dBm and range from 0 dBm to 23 dBm, i.e., $P = \{0, 1, \dots, 23\}$ dBm. On this base, the output layer consists of $24 * 2$ neurons. Unless otherwise specified, we assume that the learning rate is 0.005, the batch size is 100 and the maximum number of iterations is 5000.

Once we have adjusted the optimal weights of DNN after training phase, testing data set is adopted to verify DNN fitting results. Similarly to training phase, we input statistical CSI characteristics of previous n time slots to DNN and output predictive power allocation solutions from it. Then the output data is compared with target data to verify prediction performance of DNN.

From the discussion mentioned above, DNN-PPA algorithm to solve the power allocation problem under delayed CSI feedback in V2X scenario is summarized in Algorithm 3.

V. SIMULATION RESULTS AND PERFORMANCE ANALYSIS

In this section, we demonstrate the simulation results of PCA-PA and DNN-PPA respectively. The corresponding performances are compared with popular power allocation approaches in V2X scenario. Based on the 3GPP TR

37.885 [37], we construct a vehicle uplink communication scenario on the multi-lane highway. The BS is located at center of highway as illustrated in Fig. 1 [6]. The vehicles have initial position distributions which follow Spatial Poisson Process and move along the highway at a certain speed. In addition, each vehicle is allowed to use only one link, i.e., V2V or V2I, to propagate data. We assume that the spectrum of one CUE can only be reused by a single VUE and one VUE is only allowed to share the spectrum of a single CUE. Especially, the CUEs are assumed to have equal shares of total bandwidth and the pairing method between VUEs and CUEs is considered random. Note that delayed CSI feedback and fast time-varying channels in V2X scenario are also considered. The major simulation parameters are listed in Table 3 and the channel models for V2I and V2V links are described in Table 4. Unless otherwise specified, all parameters are set to the values in Table 3 and Table 4 by default, whereas the settings in each figure take precedence wherever applicable. In the subsequent simulations, firstly improving system throughput and satisfying QoS constraints are adopted as metrics to evaluate the PCA-PA scheme and its counterparts. Secondly, we adopt the prediction accuracy of DNN-PPA as an evaluation function in consideration of

delayed CSI feedback in V2X scenario. In addition, we compare the throughput performance between DNN-PPA algorithm and corresponding optimal solution.

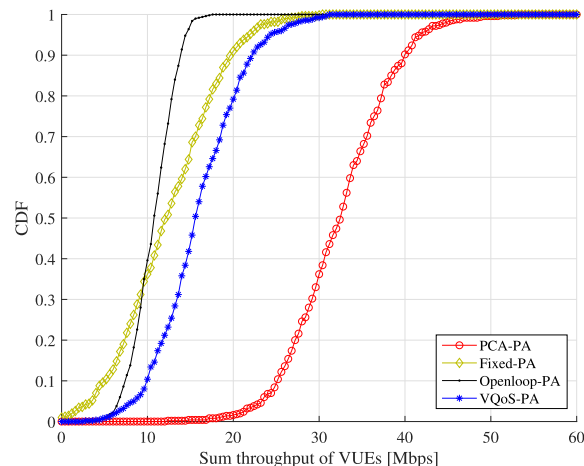
A. PERFORMANCE OF PCA-PA SCHEME

In this subsection, the performance of improving system throughput while guaranteeing QoS constraint is evaluated with MATLAB system-level simulation tools. For the sake of explanation, simulation results of three existing benchmarks and PCA-PA scheme are provided to compare their performances. After that, we analyze the impact of QoS constraint value on system throughput and feasible region classification cases in proposed PCA-PA scheme. In particular, the results in Fig. 6 are obtained from 1000 time slot realizations. Fig. 7, Fig. 8 and Fig. 9 are plotted with averaging 1000 time slot realizations for each QoS constraint value respectively.

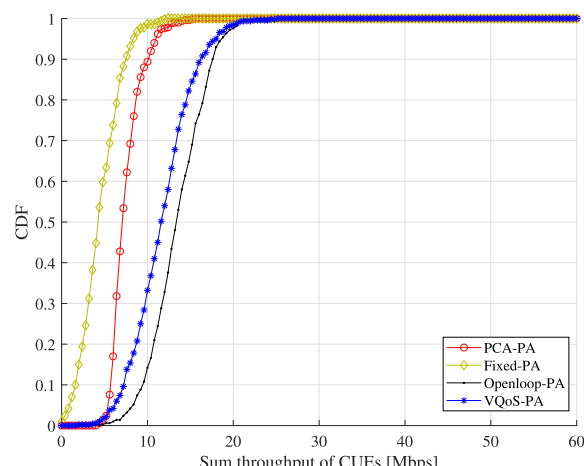
In Fig. 6, to demonstrate the superiority of proposed scheme, we compare the cumulative distribution function (CDF) of throughput achieved by PCA-PA scheme versus three benchmarks. The first benchmark is a power allocation approach developed in [6]. This approach aims to maximize throughput of CUEs while satisfying QoS constraints of VUEs, namely VQoS-PA. The open-loop power control method mentioned in [39] is adopted as the second benchmark, namely openloop-PA. It uses path loss of reference signal to adjust transmit power individually. In the last benchmark, both VUEs and CUEs select fixed maximum transmit powers for communication, namely fixed-PA.

In Fig. 6(a) and Fig. 6(b), we show the CDFs of throughput for VUEs and CUEs, respectively. We observe that the proposed PCA-PA scheme achieves strictly better performance for VUEs against benchmarks even though it is slightly worse than VQoS-PA and openloop-PA for CUEs. This can be attributed to two aspects. The first is that V2V links have shorter distances, which means advantages for communication. Therefore, in order to improve throughput, the transmit powers of VUEs tend to be maximum values in PCA-PA scheme. This causes that the PCA-PA scheme shows extremely high throughput for VUEs. The second is that compared to V2V links, most V2I links do not have communication advantages due to longer transmission distances. In consequence, on the premise of meeting QoS constraint, CUEs are inclined to decrease transmit powers to reduce interference to VUEs. This is the reason why PCA-PA is slightly worse than VQoS-PA and openloop-PA for throughput of CUEs. However, In Fig. 6(c), as we can see, the proposed PCA-PA scheme not only meets QoS constraints of all links, but also greatly improves the sum throughput of V2X system. It is consistent with the theories mentioned above.

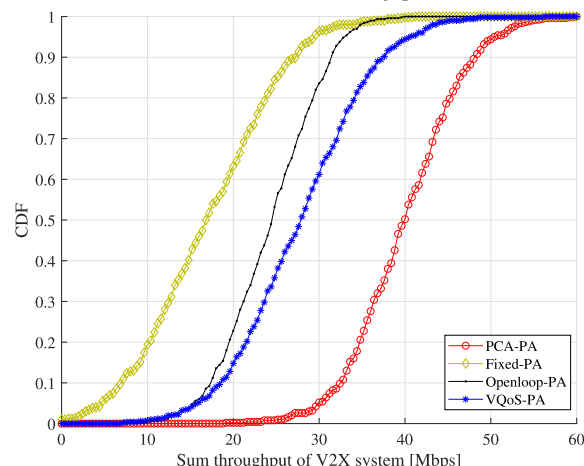
Fig. 7 shows the average throughput with a growing QoS constraint in PCA-PA scheme. From the figure, the average throughput of V2X system decreases with a growing QoS constraint. This is because as QoS constraint increases, fewer links can meet the constraint. It is also interesting to note that in Fig. 7, the average throughput shows a downward trend for CUEs and upward trend for VUEs respectively, for which the



(a) CDF of VUEs throughput.



(b) CDF of CUEs throughput.



(c) CDF of V2X system throughput

FIGURE 6. Performance of Throughput for V2X communication.

reasons are twofold. On one hand, in PCA-PA scheme, most CUEs select the transmit powers of meeting QoS constraint, thus the increasing constraint brings higher throughput for CUEs. On the other hand, the increasing transmit powers of CUEs cause higher interference and lower throughput for VUEs.

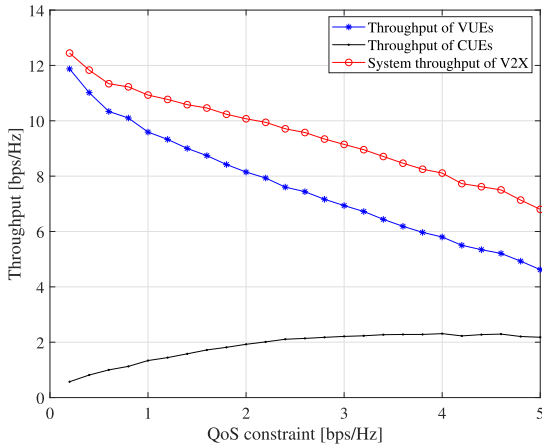


FIGURE 7. Throughput versus QoS constraint.

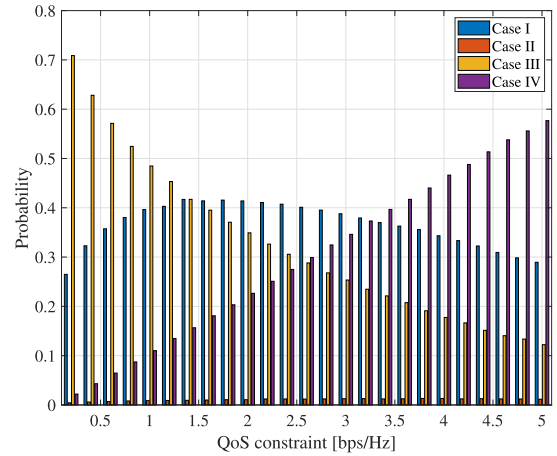


FIGURE 9. Probability of feasible region classification cases.

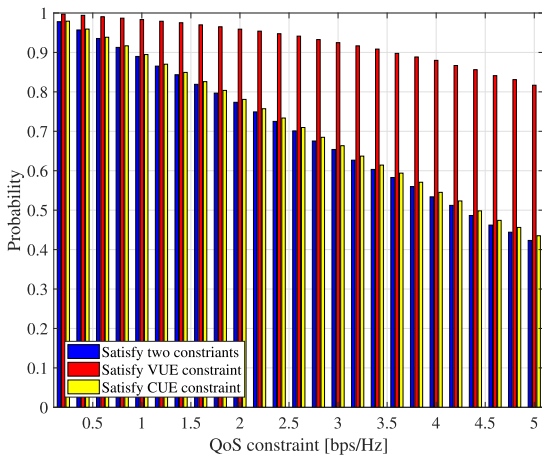


FIGURE 8. Probability of satisfying QoS constraint.

In Fig. 8, we analyze the satisfaction probability with the increasing QoS constraint for CUEs, VUEs and V2X system respectively in PCA-PA scheme. Note that the non-satisfaction probabilities are caused by harsh communication environment and strict QoS constraints. PCA-PA scheme provides the optimal solution for (5) on basis of CSI feedback, which can be deduced from the aforementioned theorems. From the figure, on one hand, the VUEs maintain a high probability of satisfying QoS constraint due to their advantages of neighbor communication. On the other hand, the satisfaction probability for CUEs gradually decreases as QoS constraint increases. This is pretty intuitive that higher constraint means more difficult to satisfy. These two aspects also make it less possible that V2X system satisfies two higher QoS constraints.

Fig. 9 shows the impact of QoS constraints on distribution probabilities of feasible region classification cases in PCA-PA scheme. As can be seen, the probability of Case III is high at a loose QoS constraint and decreases with QoS constraint becoming stricter. However, the probability of Case IV shows the opposite trend. This observation makes

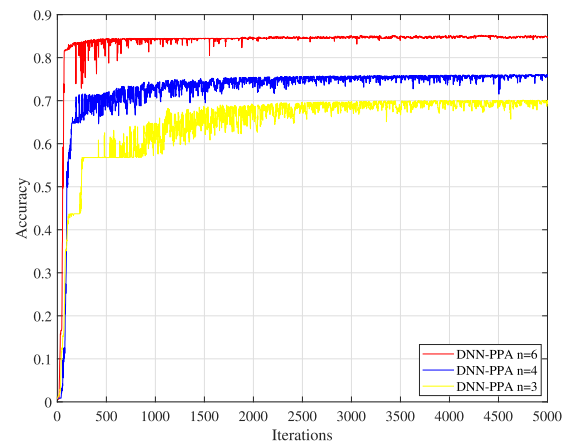
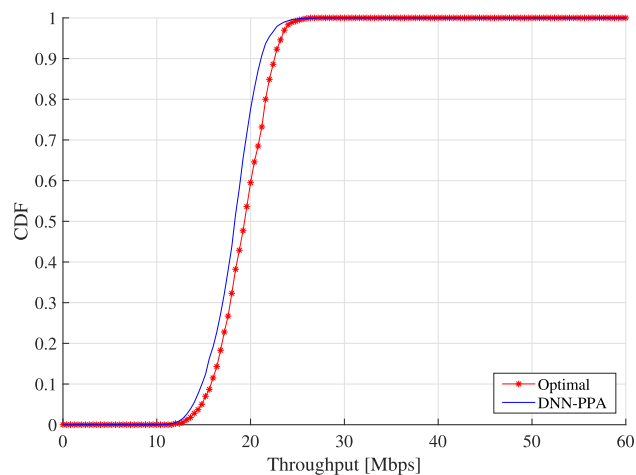


FIGURE 10. Prediction accuracy of DNN-PPA.

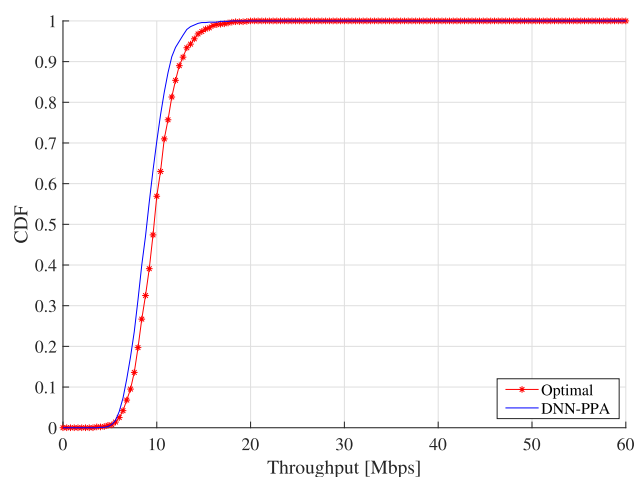
intuitive sense because Case IV, i.e., no power allocation solution for (5), increases its probability when QoS constraints become stricter. There is an interesting finding that the probability of Case I increases initially and decreases afterwards as QoS constraint increases. Additionally, Case II always keeps at a low probability no matter how the QoS constraint varies. This can be explained that compared to V2V links, V2I links have longer transmission distance and worse communication environment. As a result, the maximum transmit powers in Case II are generally not selected by CUEs.

B. PERFORMANCE OF DNN-PPA ALGORITHM

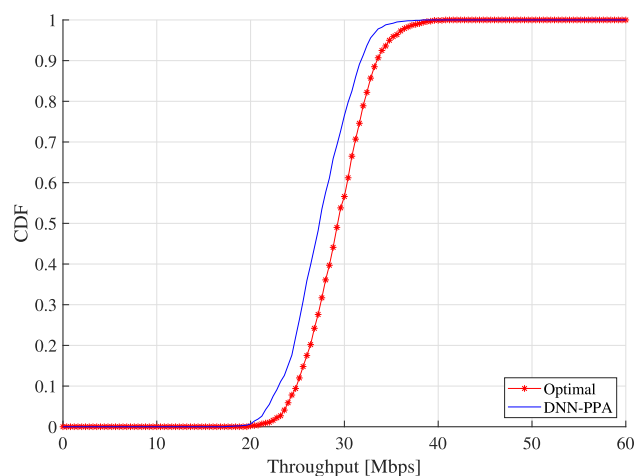
The CSI feedback in actual V2X scenario is delayed because of fast time-varying channels. As such, in this subsection we evaluate the DNN-PPA algorithm which aims to address power allocation problem under delayed CSI feedback. Especially, since we adopted the supervised learning technique, DNN-PPA approach cannot outperform the optimal solution. The prediction accuracy is adopted as metric to evaluate the proposed algorithm. Moreover, throughput performance under delayed CSI feedback of DNN-PPA algorithm and corresponding optimal solution are illustrated.



(a) Throughput of VUEs.



(b) Throughput of CUEs.



(c) Throughput of V2X system.

FIGURE 11. Throughput performance of DNN-PPA and optimal solution.

Fig. 10 demonstrates the prediction accuracy performance of DNN-PPA algorithm. In detail, we compare the impact of n , i.e., number of previous time slots for statistical CSI characteristics, on prediction accuracy. There is an encouraging finding that the prediction accuracy of DNN-PPA algo-

rithm reaches 85.71% when $n = 6$. This validates superior performance of proposed DNN-PPA algorithm to tackle the problem of delayed CSI feedback for V2X communication. We observe that when n decreases, the prediction accuracy of DNN-PPA shows a trend of gradual decline. This can be explained that few parameters fed into DNN-PPA can easily result in underfitting. In addition, it can be seen from the figure that the network converges most rapidly when $n = 6$ and most slowly when $n = 3$. This is because the statistical CSI characteristics of fewer time slots make it more difficult to map the relationship between inputs and outputs of DNN-PPA.

In Fig. 11, we depict the throughput performance under delayed CSI feedback of DNN-PPA algorithm for VUEs, CUEs and V2X system, respectively. The proposed algorithm with $n = 6$ is compared to corresponding optimal solution. From Fig. 11(a) and Fig. 11(b), the CDFs of DNN-PPA algorithm for both VUEs and CUEs are close to optimal solutions. This validates the anti-delay and fairness of proposed algorithm in V2X scenarios. As seen in Fig. 11(c), the DNN-PPA algorithm impressively has a comparable system throughput to optimal solution. This further substantiates the surprising performance of proposed DNN-PPA algorithm in solving delayed CSI feedback problem for V2X communication.

VI. CONCLUSION

In this paper, we proposed the power allocation design under delayed CSI feedback to maximize system throughput and guarantee QoS constraint for V2X communication. Firstly, we revealed the relationship between throughput performance and power allocation utilizing the PCA method. On this base, we proposed a PCA-PA scheme to maximize sum throughput of V2X system while satisfying QoS constraint of each link. Secondly, due to the fast time-varying channel caused by high-speed vehicle mobility, instantaneous CSI feedback is difficult to be tracked in practical V2X scenario. In order to address delayed CSI feedback, a DNN-PPA algorithm utilizing the statistical CSI characteristics of previous time slots was developed for V2X communication. Finally, a V2X communication model compliant with the 3GPP standard was constructed and used to validate the performances of proposed PCA-PA and DNN-PPA. Simulation results illustrated PCA-PA has superior performances compared to existing approaches. Moreover, under delayed CSI feedback in V2X scenario, DNN-PPA impressively demonstrated a comparable throughput performance compared to optimal solution.

APPENDIX A PROOF OF THEOREM 1

Given an arbitrary power allocation pattern, e.g., $(P_k, P_m) = (P_1, P_2)$, not exceeding the maximum transmit power limit. Substituting the pattern into (4), we derive the system throughput function as

$$C = \log_2(1 + \gamma_1) + \log_2(1 + \gamma_2), \quad (16)$$

where $\gamma_1 = \frac{P_1 h_{m,B}}{\sigma^2 + \rho_{m,k} P_2 h_{k,B}}$ and $\gamma_2 = \frac{P_2 h_k}{\sigma^2 + \rho_{m,k} P_1 h_{m,k}}$. When both P_1 and P_2 increase by the same multiple a ($a > 1$), system throughput function is converted to

$$C' = \log_2(1 + \gamma_1') + \log_2(1 + \gamma_2'), \quad (17)$$

where $\gamma_1' = \frac{aP_1 h_{m,B}}{\sigma^2 + \rho_{m,k} aP_2 h_{k,B}}$ and $\gamma_2' = \frac{aP_2 h_k}{\sigma^2 + \rho_{m,k} aP_1 h_{m,k}}$. To compare C and C' , we decompose them as follows.

$$\frac{P_1 h_{m,B}}{\sigma^2 + \rho_{m,k} P_2 h_{k,B}} < \frac{aP_1 h_{m,B}}{\sigma^2 + \rho_{m,k} aP_2 h_{k,B}}, \quad (18)$$

and

$$\frac{P_2 h_k}{\sigma^2 + \rho_{m,k} P_1 h_{m,k}} < \frac{aP_2 h_k}{\sigma^2 + \rho_{m,k} aP_1 h_{m,k}}. \quad (19)$$

Since the log function is monotonically increasing, $C' > C$ can be derived. We can conclude that the system throughput increases when both P_1 and P_2 increase by the same multiple a ($a > 1$) until one of them is the maximum transmit power. As a result, The optimal solution for feasible power allocation region can be given by (6) or (7).

APPENDIX B PROOF OF THEOREM 2

The optimal power allocation solution of Case I is proved as follows. It can be seen visually from Fig. 3(d) that the optimal power allocation solution lies on the boundary of feasible region, i.e., A or B in Fig. 4. As mentioned above, A and B for Case I denote (P^*_k, P_{\max}) and $(P^*_{k,B}, P_{\max})$ respectively. Derived from PCA method, we can conclude

$$C_k(P^*_k, P_{\max}) = \lambda, \quad (20)$$

and

$$C_m(P^*_{k,B}, P_{\max}) = \lambda, \quad (21)$$

where $C_m(\bullet)$ and $C_k(\bullet)$ represent the throughput function of m th CUE and k th VUE, λ is the minimum QoS constraint. Therefore, comparing the system throughput of A and B can be translated into comparison of $C_k(P^*_{k,B}, P_{\max})$ and $C_m(P^*_k, P_{\max})$, which can be demonstrated as follows. Denote $P^*_{k,B}$ as aP^*_k ($a > 1$) since $P^*_{k,B} > P^*_k$. Then $C_k(P^*_{k,B}, P_{\max})$ and $C_m(P^*_k, P_{\max})$ can be written as

$$C_k(P^*_{k,B}, P_{\max}) = \log_2\left(1 + \frac{aP^*_k h_k}{\sigma^2 + \rho_{m,k} P_{\max} h_{m,k}}\right), \quad (22)$$

and

$$C_m(P^*_k, P_{\max}) = \log_2\left(1 + \frac{P_{\max} h_{m,B}}{\sigma^2 + \rho_{m,k} P^*_k h_{k,B}}\right). \quad (23)$$

Due to $C_m(P^*_{k,B}, P_{\max}) = C_k(P^*_k, P_{\max})$, we obtain expansion forms of their SINRs, i.e., γ^B_m and γ^A_k expressed as

$$\frac{P_{\max} h_{m,B}}{\sigma^2 + \rho_{m,k} aP^*_k h_{k,B}} = \frac{P^*_k h_k}{\sigma^2 + \rho_{m,k} P_{\max} h_{m,k}}. \quad (24)$$

On this base, It can be deduced as follows.

$$a\gamma^A_k = a\gamma^B_m > \frac{P_{\max} h_{m,B}}{\sigma^2 + \rho_{m,k} P^*_k h_{k,B}}. \quad (25)$$

In summary, $C_k(P^*_{k,B}, P_{\max}) > C_m(P^*_k, P_{\max})$ thus $C(P^*_{k,B}, P_{\max}) > C(P^*_k, P_{\max})$, where $C(\bullet)$ denotes the V2X system throughput function under corresponding power allocation. Hence, the optimal power allocation solution of Case I can be written as $(P_k, P_m) = (P^*_{k,B}, P_{\max})$. Because of the symmetry of V2I links to V2V links, the optimal power allocation solution for Case II can be proved similarly. In addition, the optimal solution for Case III adopts a comparison method which does not require to be proven in detail.

REFERENCES

- [1] G. Naik, B. Choudhury, and J.-M. Park, "IEEE 802.11bd & 5G NR V2X: Evolution of radio access technologies for V2X communications," *IEEE Access*, vol. 7, pp. 70169–70184, 2019.
- [2] A. Masmoudi, S. Feki, K. Mnif, and F. Zarai, "Efficient radio resource management for D2D-based LTE-V2X communications," in *Proc. IEEE/ACS 15th Int. Conf. Comput. Syst. Appl. (AICCSA)*, Oct. 2018, pp. 1–6.
- [3] M. I. Ashraf, C.-F. Liu, M. Bennis, W. Saad, and C. S. Hong, "Dynamic resource allocation for optimized latency and reliability in vehicular networks," *IEEE Access*, vol. 6, pp. 63843–63858, 2018.
- [4] F. Abbas, P. Fan, and Z. Khan, "A novel low-latency V2 V resource allocation scheme based on cellular V2X communications," *IEEE Trans. Intell. Transp. Syst.*, vol. 20, no. 6, pp. 2185–2197, Jun. 2019.
- [5] *Technical Specification Group Radio Access Network: Study LTE-Based V2X Services: (Release 14)*, Standard 3GPP TR 36.885 V2.0.0, 3rd Generation Partnership Project, Jun. 2016.
- [6] L. Liang, G. Y. Li, and W. Xu, "Resource allocation for D2D-enabled vehicular communications," *IEEE Trans. Commun.*, vol. 65, no. 7, pp. 3186–3197, Jul. 2017.
- [7] D. Lin, Y. Tang, Y. Yao, and A. V. Vasilakos, "User-priority-based power control over the D2D assisted Internet of vehicles for mobile health," *IEEE Internet Things J.*, vol. 4, no. 3, pp. 824–831, Jun. 2017.
- [8] X. Peng, H. Zhou, B. Qian, K. Yu, F. Lyu, and W. Xu, "Enabling security-aware D2D spectrum resource sharing for connected autonomous vehicles," *IEEE Internet Things J.*, vol. 7, no. 5, pp. 3799–3811, May 2020.
- [9] T. Zhou, B. Xu, T. Xu, H. Hu, and L. Xiong, "User-specific link adaptation scheme for device-to-device network coding multicast," *IET Commun.*, vol. 9, no. 3, pp. 367–374, Feb. 2015.
- [10] Z. Wang, T. Zhou, T. Xu, and H. Hu, "An iterative greedy user clustering algorithm for D2D-relay in vehicular communication systems," *IET Microw., Antennas Propag.*, vol. 13, no. 8, pp. 1087–1095, Jul. 2019.
- [11] T. Xu, M. Zhang, and T. Zhou, "Statistical signal transmission technology: A novel perspective for 5G enabled vehicular networking," *IEEE Wireless Commun.*, vol. 24, no. 6, pp. 22–29, Dec. 2017.
- [12] C.-S. Kim, H.-J. Kim, J.-S. Lim, J.-Y. Hong, and Y. Chong, "Measurement results of high-speed V2X channel characteristics in expressway environment," in *Proc. Int. Symp. Antennas Propag. (ISAP)*, Oct. 2018, pp. 1–2.
- [13] X. Shu, C. Li, W. Chen, J. Yu, and K. Yang, "Performance analysis of V2 V radio channel under typical urban intersection scenario," in *Proc. IEEE Int. Conf. Commun. Syst. (ICCS)*, Dec. 2018, pp. 216–220.
- [14] M. Botsov, M. Klügel, W. Kellerer, and P. Fertl, "Location dependent resource allocation for mobile device-to-device communications," in *Proc. IEEE Wireless Commun. Netw. Conf. (WCNC)*, Apr. 2014, pp. 1679–1684.
- [15] W. Sun, E. G. Ström, F. Brannström, K. C. Sou, and Y. Sui, "Radio resource management for D2D-based V2 V communication," *IEEE Trans. Veh. Technol.*, vol. 65, no. 8, pp. 6636–6650, Aug. 2016.
- [16] X. Tao, C. Jiang, J. Liu, A. Xiao, Y. Qian, and J. Lu, "QoE driven resource allocation in next generation wireless networks," *IEEE Wireless Commun.*, vol. 26, no. 2, pp. 78–85, Apr. 2019.
- [17] X. Li, L. Ma, Y. Xu, and R. Shankaran, "Resource allocation for D2D-based V2X communication with imperfect CSI," *IEEE Internet Things J.*, vol. 7, no. 4, pp. 3545–3558, Apr. 2020.
- [18] C. Guo, L. Liang, and G. Y. Li, "Resource allocation for V2X communications: A large deviation theory perspective," *IEEE Wireless Commun. Lett.*, vol. 8, no. 4, pp. 1108–1111, Aug. 2019.
- [19] B. Jia, H. Hu, Y. Zeng, T. Xu, and H.-H. Chen, "Joint user pairing and power allocation in virtual MIMO systems," *IEEE Trans. Wireless Commun.*, vol. 17, no. 6, pp. 3697–3708, Jun. 2018.

- [20] Y. Wang, Z. Yang, Y. Pan, and M. Chen, "Joint power control and user pairing for ergodic capacity maximization in V2V communications," in *Proc. 9th Int. Conf. Wireless Commun. Signal Process. (WCSP)*, Oct. 2017, pp. 1–6.
- [21] Y. Ren, F. Liu, Z. Liu, C. Wang, and Y. Ji, "Power control in D2D-based vehicular communication networks," *IEEE Trans. Veh. Technol.*, vol. 64, no. 12, pp. 5547–5562, Dec. 2015.
- [22] Z. Liu, X. Han, Y. Liu, and Y. Wang, "D2D-based vehicular communication with delayed CSI feedback," *IEEE Access*, vol. 6, pp. 52857–52866, 2018.
- [23] X. Lin, J. Wu, S. Mumtaz, S. Garg, J. Li, and M. Guizani, "Blockchain-based on-demand computing resource trading in IoV-assisted smart city," *IEEE Trans. Emerg. Topics Comput.*, early access, Feb. 6, 2020, doi: 10.1109/TETC.2020.2971831.
- [24] H. Liang, J. Wu, S. Mumtaz, J. Li, X. Lin, and M. Wen, "MBID: Micro-blockchain-based geographical dynamic intrusion detection for V2X," *IEEE Commun. Mag.*, vol. 57, no. 10, pp. 77–83, Oct. 2019.
- [25] S. Khan, H. A. Khattak, A. Almogren, M. A. Shah, I. Ud Din, I. Alkhalifa, and M. Guizani, "5G vehicular network resource management for improving radio access through machine learning," *IEEE Access*, vol. 8, pp. 6792–6800, 2020.
- [26] C. Jiang, H. Zhang, Y. Ren, Z. Han, K.-C. Chen, and L. Hanzo, "Machine learning paradigms for next-generation wireless networks," *IEEE Wireless Commun.*, vol. 24, no. 2, pp. 98–105, Apr. 2017.
- [27] H. Huang, S. Guo, G. Gui, Z. Yang, J. Zhang, H. Sari, and F. Adachi, "Deep learning for physical-layer 5G wireless techniques: Opportunities, challenges and solutions," *IEEE Wireless Commun.*, vol. 27, no. 1, pp. 214–222, Feb. 2020.
- [28] T. Xu, T. Zhou, J. Tian, J. Sang, and H. Hu, "Intelligent spectrum sensing: When reinforcement learning meets automatic repeat sensing in 5G communications," *IEEE Wireless Commun.*, vol. 27, no. 1, pp. 46–53, Feb. 2020.
- [29] X. Shang, H. Hu, X. Li, T. Xu, and T. Zhou, "Dive into deep learning based automatic modulation classification: A disentangled approach," *IEEE Access*, vol. 8, pp. 113271–113284, 2020.
- [30] S. Han, Y. Oh, and C. Song, "A deep learning based channel estimation scheme for IEEE 802.11p systems," in *Proc. IEEE Int. Conf. Commun. (ICC)*, May 2019, pp. 1–6.
- [31] S. Khan, K. Muhammad, S. Mumtaz, S. W. Baik, and V. H. C. de Albuquerque, "Energy-efficient deep CNN for smoke detection in foggy IoT environment," *IEEE Internet Things J.*, vol. 6, no. 6, pp. 9237–9245, Dec. 2019.
- [32] S. Zafar, S. Jangsher, O. Bouachir, M. Aloqaily, and J. Ben Othman, "QoS enhancement with deep learning-based interference prediction in mobile IoT," *Comput. Commun.*, vol. 148, pp. 86–97, Dec. 2019.
- [33] H. Ye, G. Y. Li, and B.-H.-F. Juang, "Deep reinforcement learning based resource allocation for V2V communications," *IEEE Trans. Veh. Technol.*, vol. 68, no. 4, pp. 3163–3173, Apr. 2019.
- [34] H. Lee, S. H. Lee, and T. Q. S. Quek, "Deep learning for distributed optimization: Applications to wireless resource management," *IEEE J. Sel. Areas Commun.*, vol. 37, no. 10, pp. 2251–2266, Oct. 2019.
- [35] J. Gao, M. R. A. Khandaker, F. Tariq, K.-K. Wong, and R. T. Khan, "Deep neural network based resource allocation for V2X communications," in *Proc. IEEE 90th Veh. Technol. Conf. (VTC-Fall)*, Sep. 2019, pp. 1–5.
- [36] X. Tao, Y. Duan, M. Xu, Z. Meng, and J. Lu, "Learning QoE of mobile video transmission with deep neural network: A data-driven approach," *IEEE J. Sel. Areas Commun.*, vol. 37, no. 6, pp. 1337–1348, Jun. 2019.
- [37] *Technical Specification Group Radio Access Network: Study on evaluation methodology of New Vehicle-to-Everything (V2X) use Cases for LTE and NR: (Release 15)*, Standard 3GPP TR 37.885 V15.2.0, 3rd Generation Partnership Project, Dec. 2018.
- [38] *Technical Specification Group Radio Access Network: Study on Channel Model for Frequencies From 0.5 to 100 GHz (Release 16)*, Standard 3GPP TR 38.901 V16.0.0, 3rd Generation Partnership Project, Oct. 2019.
- [39] *Technical Specification Group Radio Access Network: Evolved Universal Terrestrial Radio Access (E-UTRA): Physical Layer Procedures (Release 15)*, Standard 3GPP TS 36.213 V15.8.0, 3rd Generation Partnership Project, Dec. 2019.
- [40] K. J. Ahmed and M. J. Lee, "Secure LTE-based V2X service," *IEEE Internet Things J.*, vol. 5, no. 5, pp. 3724–3732, Oct. 2018.
- [41] J.-Y. Hwang, M. Jung, and S.-W. Lee, "LTE based V2X receiver to support high speed," in *Proc. Int. Conf. Inf. Commun. Technol. Converg. (ICTC)*, Oct. 2017, pp. 747–749.



JIAN SANG received the B.S. degree in communication engineering from Northeastern University, China, in 2018. He is currently pursuing the joint M.S. degree with the Shanghai Advanced Research Institute, Chinese Academy of Sciences, and Shanghai University. His research interests include machine learning and vehicle-to-everything in wireless communications.



TING ZHOU (Member, IEEE) received the B.S. and M.S. degrees from the Department of Electronic Engineering, Tsinghua University, in 2004 and 2006, respectively, and the Ph.D. degree from the Shanghai Institute of Microsystem and Information Technology (SIMIT), Chinese Academy of Sciences, in 2011. She is currently a Full Professor with the Shanghai Advanced Research Institute, CAS. She has coauthored more than 20 technical journals and conferences, and 49 granted or filed patents. Her research interests include wireless resource management and mobility management, intelligent networking of heterogeneous wireless networks, and 5G mobile systems. She has received the 2016 and 2015 First Prize of the Technological Invention Award from the China Institute of Communications and the 2015 Second Prize of the Shanghai Science and Technology Progress Award.



TIANHENG XU (Member, IEEE) received the Ph.D. degree from the Shanghai Institute of Microsystem and Information Technology, Chinese Academy of Sciences, Shanghai, China, in 2016. He is currently an Associate Professor with the Shanghai Advanced Research Institute, Chinese Academy of Sciences. His main research interests include 5G wireless communications, spectrum sensing technologies, statistical signal transmission technologies, and vehicular communication technologies. He received the President Scholarship of Chinese Academy of Sciences (First Grade), in 2014, the Outstanding Ph.D. Graduates Award of Shanghai, in 2016, and the Best Paper Award at the IEEE GlobeCom 2016.



YANLIANG JIN (Member, IEEE) received the B.S. and M.S. degrees in electrical engineering from Xidian University, Xi'an, China, in 1997 and 2000, respectively, and the Ph.D. degree in communication and information system from Shanghai Jiao Tong University, in 2005. He is currently an Associate Professorship with the School of Communication and Information Engineering (SCIE), Shanghai University (SHU). He has published more than 30 journal articles/conference papers. His research interests include mobile ad hoc networks (MANETs), wireless sensor networks (WSNs), wireless multimedia sensor networks (WMSNs), wireless broadband access, and signal processing.



ZHENGHANG ZHU received the M.S. degree in information and communication engineering from Tsinghua University, in 2008. His main research interests include software defined radio, next-generation wireless networks, and V2X.

• • •